Desalination and Water Treatment
www.deswater.com

doi: 10.5004/dwt.2018.22228

110 (2018) 154–167
April

Chemically modified bentonite/Fe_3O_4 nanocomposite for Pb(II), Cd(II), and Ni(II) removal from synthetic wastewater

Fatemeh Ahmadi, Hossein Esmaeili*

Department of Chemical Engineering, Bushehr Branch, Islamic Azad University, Bushehr, Iran, Tel. +989179885692; Fax: +987735683700; emails: esmaeili.hossein@gmail.com (H. Esmaeili), fatemeh_ahmadi1993@yahoo.com (F. Ahmadi)

Received 27 September 2017; Accepted 18 March 2018

ABSTRACT

In this study, bentonite/Fe_3O_4 nanocomposite was synthesized via a chemical coprecipitation method using NaOH as the precipitating agent. The obtained bio-adsorbent was used for cadmium, lead, and nickel removal from aqueous solutions. The physical and chemical properties of bentonite/magnetite nanocomposite (BMNC) were studied using Brunauer, Emmett and Teller; scanning electron microscope; Fourier-transform infrared spectroscopy; X-ray diffraction, X-ray fluorescence; and dynamic light scattering. In this work, the effect of different parameters such as pH, temperature, contact time, initial concentration, and BMNC dose was examined on the removal of Cd(II), Pb(II), and Ni(II) ions from aqueous solution. The uptake rate of metal ions on the BMNC was rapid. Kinetics behavior of bio-adsorption showed that pseudo-second-order model can describe the kinetics of the adsorption process better than pseudo-first-order model. To investigate the equilibrium behavior of adsorption, Langmuir, Freundlich, and Dubinin–Radushkevich (D–R) isotherm models were investigated and D–R isotherm exhibited the best fit with the experimental data. The maximum bio-adsorption capacities by Langmuir model were 9.4339, 108.695, and 5.9808 mg/g for cadmium, lead, and nickel, respectively. In addition, adsorption onto BMNC follows a physical mechanism. Furthermore, the thermodynamic study showed that adsorption process was spontaneous and exothermic.

Keywords: Adsorbent; Bentonite/Fe_3O_4 nanocomposite; Heavy metal ions; Aqueous solution

1. Introduction

Heavy metal pollutants are generated by natural processes and human activities. Due to the amount, duration, and toxicity of pollutants in aqueous solution, the metal ions are extremely harmful to human life [1]. Toxic heavy metals in water can infiltrate the food chain through different ways such as drinking water, food, and breathing airborne particles enter the human body [2]. The main heavy metals associated with environmental contamination, and which offer potential danger to the ecosystem, are lead (Pb), cadmium (Cd), and nickel (Ni) [3]. These metals are being used widely in industries such as electroplating, steel, battery, paint, and pigment. Because of their toxicity, the presence of these metal ions in high quantities will interfere with many beneficial uses of water and may threaten aquatic life. So, the removal of these metals from water and wastewater is necessary [4,5]. To attenuate heavy metals from wastewater, we can use different methods, such as coagulation, chemical oxidation, membrane filtration, electro-dialysis, reverse osmosis, and chemical precipitation. These methods have not been very successful because of high capital and operational costs. Adsorption technique is an attractive method for water treatment with the advantages of high treatment efficiency and no harmful by-product to treat water and because of the remarkable advantages like availability, profitability, ease of operation, and effectiveness than other techniques [5–10]. Nanostructured adsorbents have strong effects for treatment of contaminants from wastewaters due to a large specific surface area, high adsorption capacities, and short diffusion paths [11,12]. However, it is difficult for

* Corresponding author.

recovery of nanosized adsorbents from aqueous media [13,14]. The application of nanostructured magnetic adsorbents (such as, Fe_3O_4 nanoparticles) is a new technology which has recently received important attention; because of their potency to be easily separated from wastewater using an external magnetic field after adsorption, in this way, their reconstruction and reuse are essential. For practical application of nanoparticles in various potential fields, their surface modification is vital [15]. To improve the magnetic features of iron oxide, we can combine magnetic nanoparticles with different materials such as clay, CaO, MgO, etc. Different methods such as impregnation, ball milling, and chemical coprecipitation have been expanded to combine them together to produce magnetic nanocomposite. Among them, chemical coprecipitation is the most important method because of simple procedure and no need of special chemicals [5,6].

Clay (such as bentonite) is found naturally on the surface of the earth composed mainly of silica, alumina, water, and weathered rock. For over a decade, clay is a matter of much attention due to its use as an effective adsorbent to remove heavy metal ions from water. Natural clays are low cost, with high surface area and a net negative charge on their structure, which attracts cations like heavy metals [8,16,17].

Many researchers have been worked on the removal of heavy metals by means of CaO/Fe_3O_4 [5], $MnFe_2O_4$/bentonite nanocomposite [6], Fe_3O_4/bentonite nanocomposite [16], and clay ferrite nanocomposite [18], and their results have cleared the use of this adsorbents are very effective on the removal of heavy metals from aqueous solutions.

The main aim of this research was to investigate the new chemically modified bentonite/magnetite nanocomposite (BMNC) as an effective bio-sorbent for the removal of Cd, Ni, and Pb ions from aqueous solution. To do this, the effect of several parameters such as temperature, pH, time, adsorbent dosage, and ion concentrations were investigated. Also, equilibrium, kinetic, and thermodynamic studies were done.

2. Materials and methods

2.1. Chemicals

Ferric chloride ($FeCl_3.6H_2O$), Ferrous chloride ($FeCl_2.4H_2O$), $Pb(NO_3)_2$, $Ni(NO_3)_2.4H_2O$, $Cd(NO_3)_2.4H_2O$, HCl, and NaOH were purchased from Merck company (Germany).

2.2. Preparation of stock solutions

A preliminary stock solution of lead, cadmium, and nickel with 1,000 mg/L concentration was prepared through a dissolution of $Pb(NO_3)_2$, $Cd(NO_3)_2{\cdot}4H_2O$, and $Ni(NO_3)_2.4H_2O$, respectively in deionized distilled water. Solutions with required initial concentrations were prepared by diluting the base solution with double-distilled water. The pH of the working solution was set by 1 M NaOH and HCl. Measurement of pH was performed by digital pH meter (Metrohm 744, Switzerland).

2.3. Preparation of Fe_3O_4

Fe_3O_4 was prepared by using chemical coprecipitation method. To do this, 2 mmol $FeCl_2.4H_2O$ and 4 mmol $FeCl_3.6H_2O$ were dissolved in the distilled water; then under vigorous magnetic shaking at 70°C, NaOH solution was added dropwise to increase the solution pH to 10 and the mixing continued for 1 h. After cooling down, the gathered Fe_3O_4 was washed several times with distilled water and dried in an oven at 105°C for 2 h [16].

2.4. Preparation of bentonite/magnetic nanocomposite

The bentonite was added into a solution containing 2 mmol $FeCl_2.4H_2O$ and 4 mmol $FeCl_3.6H_2O$ at ambient temperature. The amount of bentonite was adjusted to obtain Fe_3O_4/bentonite mass ratio of 1:10 under severe magnetic mixing, the pH was slowly raised by adding NaOH solution drop by drop to 10 and stirring continued for 50 min and stirring was then stopped. The suspension was heated to 95°C–110°C for 2 h. After cooling, the prepared magnetic composite was repeatedly washed with distilled water. Upon completion of the oxidation reaction, the product was separated from the solution using a magnetic field and washed with distilled water. The obtained materials were then separated from water and dried in an oven at 100°C for 24 h. After cooling, the product is pulverized by a mill [16].

2.5. Analysis methods

The amount of Ni(II), Cd(II), and Pb(II) in aqueous solutions was measured by using flame atomic absorption spectrometry (Varian Spectr-AA10, Australia) before and after considered time which used air acetylene as fuel. In order to study surface changes of bentonite/magnetic composite before and after ion adsorption, scanning electron microscope (SEM, VEGA, TESCAN, Czech Republic) was used. In addition, to specify the functional groups and bio-adsorbents features, FTIR device (Perkin Elmer Spectrum Two Spectrometer, UK) was used. Moreover, Brunauer, Emmett and Teller (ASAP2020 analyzer), XRF (X-ray fluorescence, Spectro iQ, USA), XRD (X-ray diffractometer, Bruker AXS-D8 advance, Germany), and Zeta Plus (Brookhaven, USA) are applied for measuring the morphology, elemental analysis, structure features, and particle size distribution of the BMNC adsorbent.

2.6. Adsorption experiments

The adsorption of Ni(II), Cd(II), and Pb(II) from aqueous solution using BMNC was done discontinuously, and the effect of different parameters such as the contact time (5–120 min), pH (2–11), sorbent dosage (0.5–25 g/L), temperature (25°C–55°C), and the initial concentration of metal ions (5–50 mg/L) were studied. Each experiment was repeated two times, and the average result was given.

After adsorption reached equilibrium, BMNC was easily removed through an external magnetic field and the solution was gathered for metal ion concentration measurement. Residual lead, nickel, and cadmium were measured by spectrophotometry. In order to determine removal efficiency of ions from aqueous solutions, Eq. (1) was used [5]:

$$\%\ \text{Adsorption} = \frac{(C_i - C_o)}{C_i} \times 100 \quad (1)$$

The adsorption capacity of metal ions, q_e (mg/g), was also determined by Eq. (2):

$$q_e = \frac{(C_i - C_o)V}{W} \quad (2)$$

where C_i and C_o refer to the initial and equilibrium concentrations (mg/L) of metal ions, respectively. Also, V (L) and W (g) are the adsorption amount at equilibrium state, the volume of solution, and the dry weight of BMNC, respectively.

3. Results and discussion

3.1. Characterization of adsorbents

The SEM images of the adsorbent surface before and after adsorption are shown in Fig. 1.

As shown in Fig. 1(a) for the BMNC, heterogeneous surfaces with high various roughness can be seen. Also, Fig. 1(b) shows the SEM image of Fe_3O_4 nanoparticles. In Fig. 1(c) after precipitation of Fe_3O_4 onto bentonite surface, roughness and surface area of the adsorbent were increased. After adsorption as shown in Figs. 1((d)–(f)), there is a change in the morphology of the material surface (less irregular) because of adsorption between functional groups of BMNC and metal ions.

Also, the adsorbent was found to have a BET surface area of 52.1856 m^2/g and 105.4410 m^2/g, and average pore diameter of 50.38 and 96.14 Å and total pore volume of 0.094 and 0.178 cm^3/g for bentonite and BMNC, respectively.

The chemical composition of bentonite and BMNC using XRF is illustrated in Table 1. Table 1 indicates the presence of silica and alumina as major constituents of bentonite and silica and Fe_3O_4 as major constituents of BMNC. Other constituents are in the form of impurities.

Fig. 2 shows FT-IR spectra of bentonite, Fe_3O_4, BMNC, BMNC with lead, BMNC with nickel, and BMNC with cadmium. Also, functional groups at different wavenumber are given in Table 2. As illustrated in this table, adsorbent has the functional group including N–H, C–H, C=C, C–I, C–F, and C–Br at different wavenumbers and after adsorption of metal ions, the functional groups such as S=O, =C–H, C–O, and C=O can be also observed. Also, a peak is seen in the wavenumber of 3383 cm^{-1} which is mainly due to the intramolecular hydrogen bonding in magnetic particles [19]. Additionally, one peak related to NH_2 and two peaks related to Fe–O are seen in the wavenumbers of 1625, 582 and 444 cm^{-1}, respectively [16,20].

XRD analysis was performed on samples of bentonite and BMNC which is illustrated in Fig. 3. XRD pattern was plotted by X-pert software, and XRD lines were indexed. Peaks of Fe_3O_4, SiO_2, and Al_2O_3 compounds observed were matched with reference card number 0449-075-01, 2466-083-01, and 1212-046-00, respectively. Also, in XRD analysis of Fe_3O_4 nanoparticles structure, the peaks are seen at different angles such as 18.40°, 30.15°, 35.52°, 43.18°, 53.54°, 57.20°, 63.15°, and 75.03°, which are related to the crystalline phases like (111), (220), (311), (400), (422), (511), (440), and (622) [21].

The dynamic light scattering (DLS) measurements reveal particles size distribution of bentonite and BMNC which are shown in Fig. 4. As clear in this Fig., the average sizes of particles are 54.7 and 64.5 nm, for bentonite and BMNC, respectively.

3.2. Effect of pH

The impact of pH value on the adsorption of Pb(II), Ni(II), and Cd(II) onto BMNC is displayed in Fig. 5 by changing pH from 2 to 11, and the rest of the parameters were kept constant (adsorbent dosage, 1 g/L; contact time, 60 min; temperature, 25°C; initial metal ions concentration, 5 mg/L; and mixing speed, 200 rpm).

This result indicates that there was an increase in adsorption efficiency with increasing pH from 2 to 6. At low pH values, H^+ ion concentration is much more than the metal ion, in this case, H^+ ion competes with heavy metal ions to locate on active sites of adsorbent and creates repulsive force by locating on the adsorbent surface which prevents locating ions on the adsorbent surface. By increasing pH, H^+ ion concentration decreases in solution and, therefore, enough surface is created to locate heavy metal ions on the adsorbent [22]. So, the adsorption efficiency increases. The maximum uptake of the pb^{2+}, Ni^{2+}, and Cd^{2+} take place at pH value of 6. At pH > 6, adsorption of lead, nickel, and cadmium was then decreased because at high pH, the OH^- ion concentration increases in the solution, the OH^- ion forms a complex with the metal ions which finally causes the metal ions sediment in the solution and prevents them to contact with active sites; therefore, the metal ions adsorption efficiency decreases [22]. So, the highest amount of these metal ions removal was 95.66, 93.61, and 94.232, respectively. It was noticed that when the pH value was higher than 5, the sorption amount increased dramatically; this was attributed to the fact that heavy metal ions started to precipitate, reduces metal ions in water at higher pH values [23]. So, the optimal value of pH 6 was obtained.

3.3. Effect of temperature and contact time

To evaluate the effect of contact time on the adsorption efficiency, the contact time in the range of 5, 10, 15, 20, 30, 40, 60, 80, 100, and 120 min was studied. Figs. 6–8 show the impact of time on the removal of Pb(II), Cd(II), and Ni(II) using BMNC. As can be seen, the removal efficiency of the metal ion by the BMNC initially increased rapidly, so, the optimal contact time is considered 20 min for lead and cadmium and 30 min for the nickel.

Temperature is also known as an important factor in adsorption processes [24,25]. As shown in all figures, by increasing temperature from 25°C to 55°C, the removal percentage of cadmium, lead, and nickel is declined, so the optimum temperature determined 25°C. Reduction in the removal efficiency of Pb(II), Cd(II), and Ni(II) by increasing the solution temperature can be attributed to a number of reasons such as:

(1) increase in the inclination of ions to separate from the adsorbent surface and release to the bulk solution, (2) deactivating some of the active sites on the adsorbent surface due to the chemical bonds rupture, and (3) weakening the adsorption forces between the heavy metals species and active sites of adsorbent [24,25].

The results also clear that the adsorption process of cadmium, lead, and nickel ions on the surface of BMNC is exothermic.

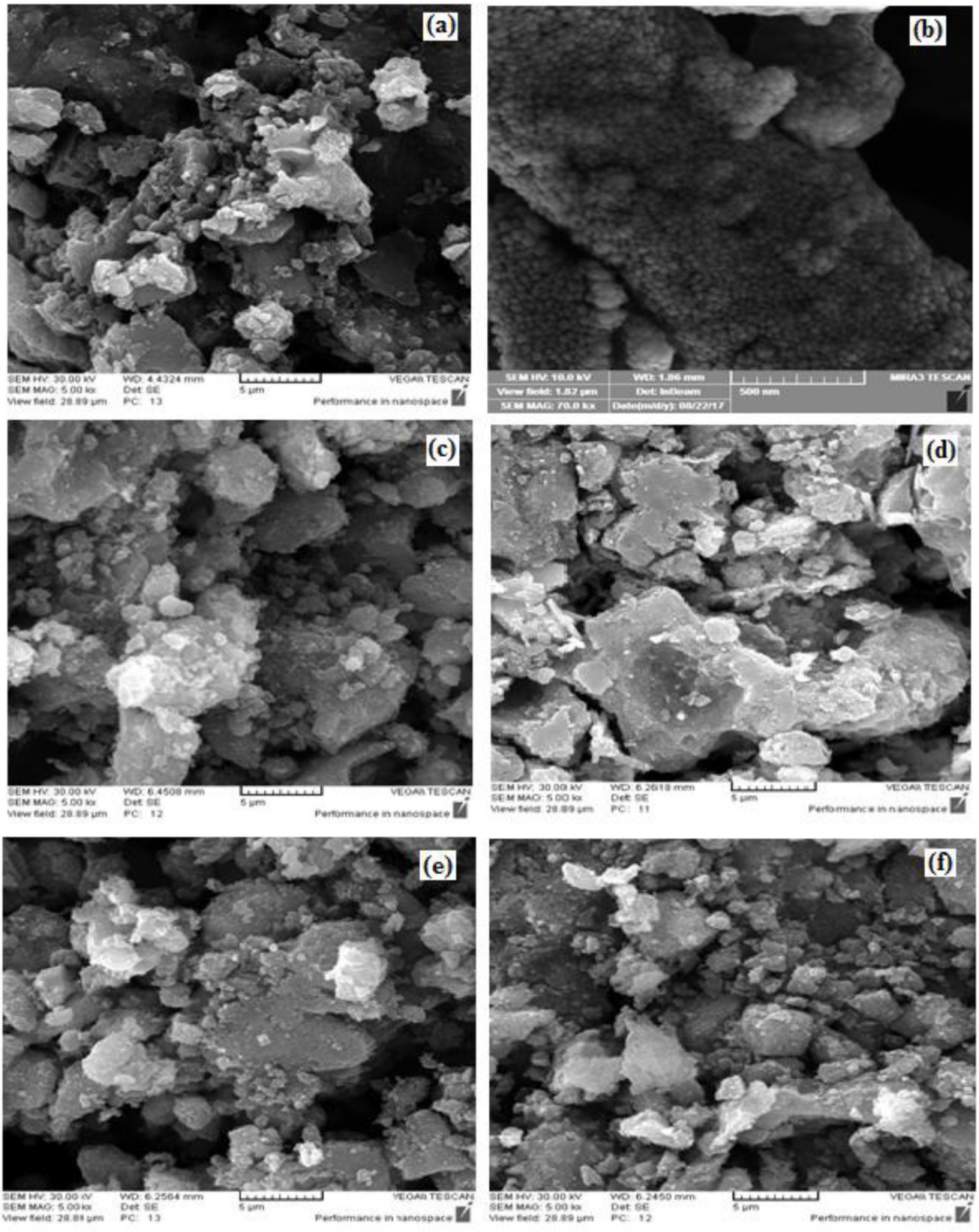

Fig. 1. SEM images of (a) bentonite, (b) Fe_3O_4, (c) BMNC before adsorption of metal ions, (d) adsorbent after adsorption of lead ions, (e) adsorbent after adsorption of nickel ions, and (f) adsorbent after adsorption of cadmium ions.

Table 1
XRF analysis of bentonite and BMNC

Sample	SiO_2	Al_2O_3	Fe_2O_3	CaO	Na_2O	MgO	K_2O	TiO_2	MnO	P_2O_5	Fe_3O_4	SO_3	LiO
Bentonite	57.75	19.8	5.34	1.94	1.051	1.97	1.34	0.67	0.105	0.169	1.633	0.51	9.49
BMNC	21.68	8.08	4.72	3.51	1.336	1.22	0.62	0.28	0.243	0.063	50.84	0.36	11.26

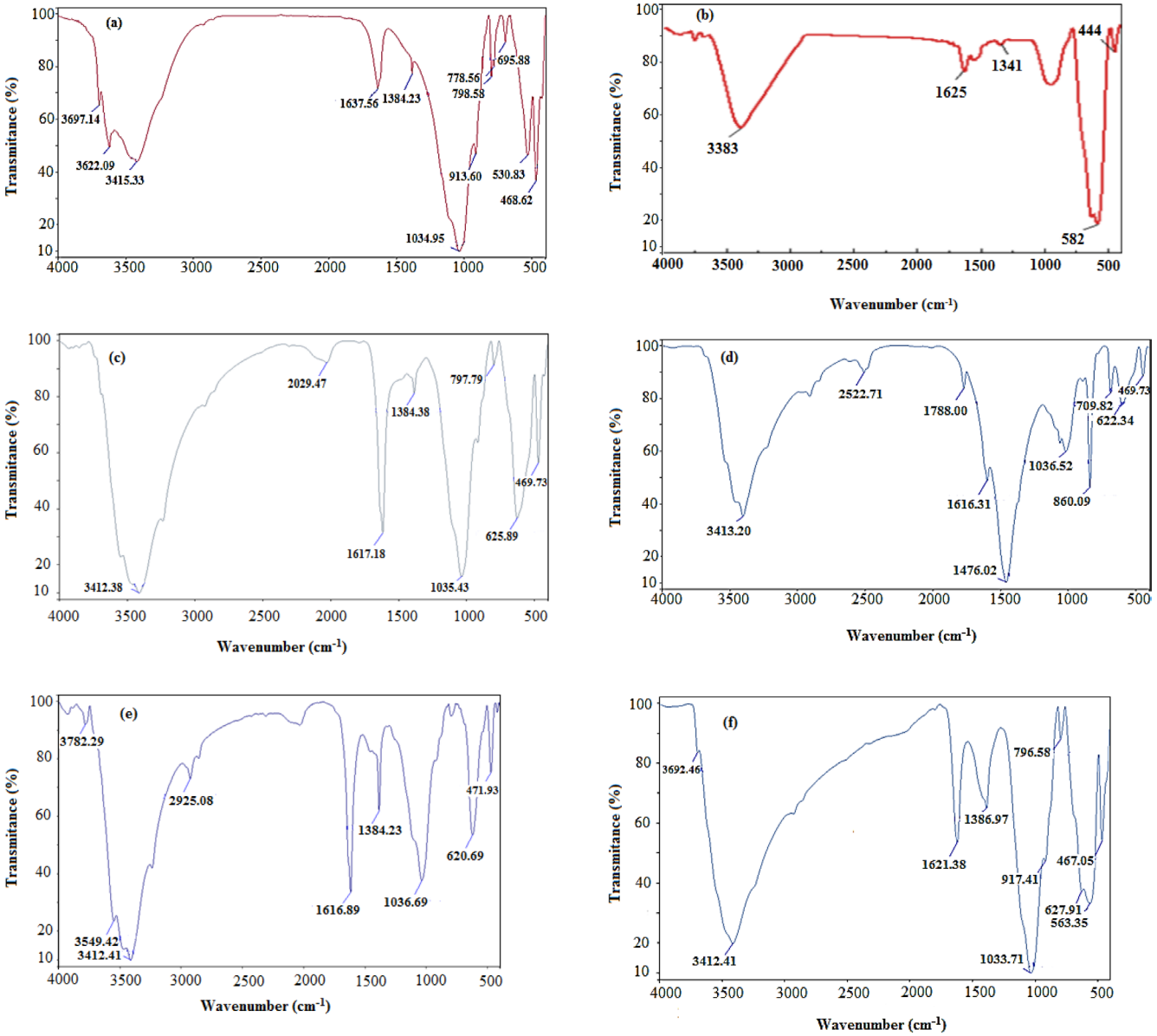

Fig. 2. FTIR analysis of (a) bentonite, (b) Fe_3O_4, (c) BMNC, (d) BMNC + lead, (e) BMNC + nickel, and (f) BMNC + cadmium.

3.4. Effect of metal ion concentration

The effect of initial concentration of lead, cadmium, and nickel ions (5, 10, 15, 20, 30, 40, and 50 mg/L) on the adsorption capacity using BMNC is shown in Fig. 9.

The results clear that at low concentrations, the adsorption capacity is low and by increasing the initial concentration of ions, the ion adsorption capacity increases. With increasing initial concentration of metal ions, they collide with each other more and infiltration into BMNC adsorbent been made easier so that adsorption capability is increased. The highest bio-adsorption performance achieved 95.6% at a concentration of 50 mg/L of metal ions.

3.5. Effect of adsorbent dosage

The sorbent dosage is an important parameter because this parameter defines the capacity of adsorbent [22]. The effect of sorbent dosage on the removal percentage of all three ions is shown in Fig. 10. First, by adding BMNC adsorbent

Table 2
FTIR spectra of adsorbent before and after adsorption of Cd(II), Ni(II), and Pb(II)

Functional group	Bentonite	BMNC	BMNC with cadmium	BMNC with nickel	BMNC with lead
	Peak (cm^{-1})	Peak (cm^{-1})	Peak (cm^{-1})	Peak (cm^{-1})	Peak (cm^{-1})
N–H	3,697.14	3,412.28	–	–	860.09
	3,415.33	797.79			709.82
	695.88				
O–H	3,622.09	–	3,692.48	3,782.29	3,413.20
	913.60		3,412.41	3,412.41	2,622.71
			917.41		
C–H	1,383.23	2,029.47	–	1,384.23	1,476.02
	798.58	1,384.38			
	778.56				
C=C	1,637.56	1,617.18	1,621.38	1,616.89	1,616.31
			796.68		
C–I	530.83	469.73	563.35	471.93	469.73
	468.62		467.05		
C–F	1,034.95	1,035.43	–	1,038.69	1,036.52
C–Br	–	625.89	627.91	620.69	622.34
S=O	–	–	1,336.97	–	–
C–O	–	–	1,033.71	–	–
=C–H	–	–	–	2,925.08	–
C=O	–	–	–	–	1,788

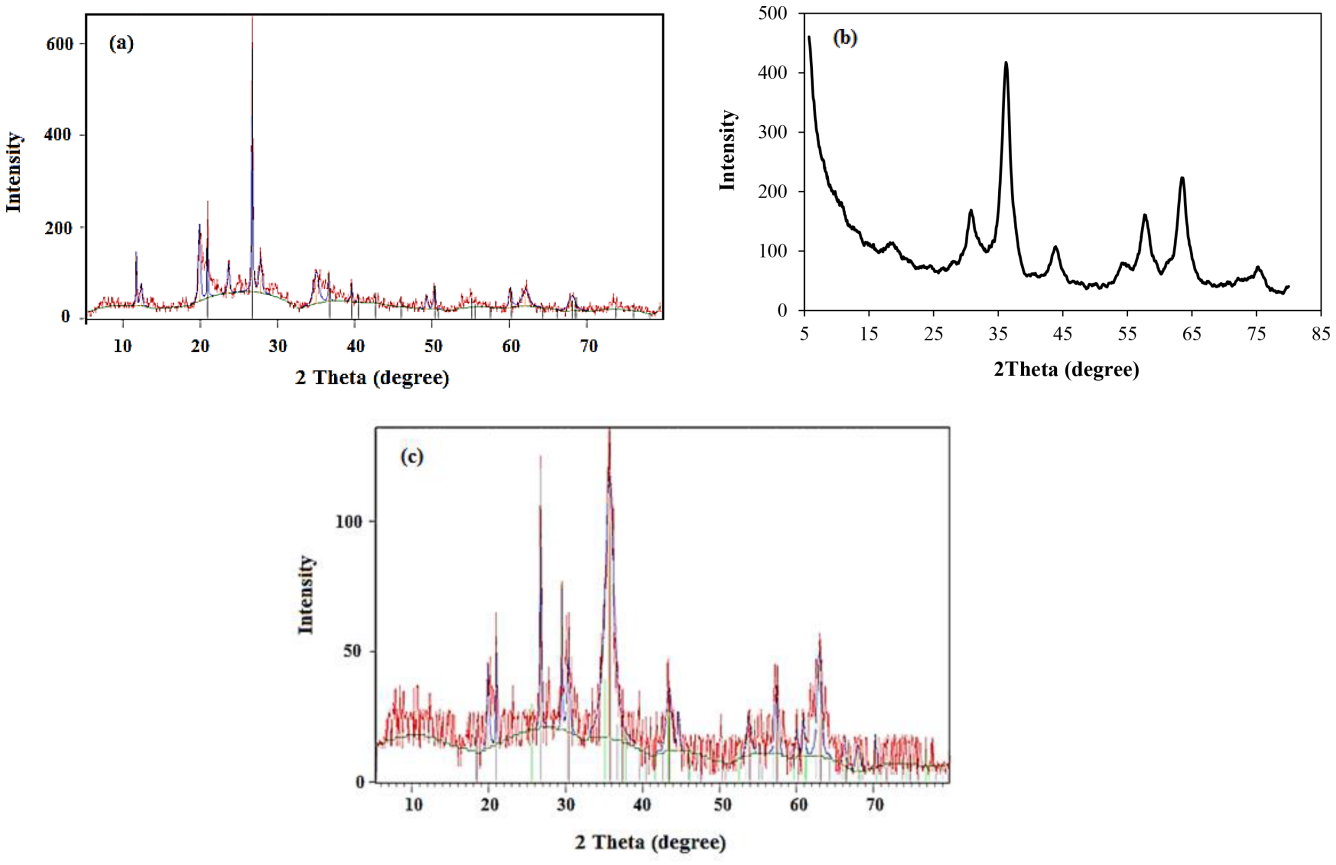

Fig. 3. XRD analysis of (a) bentonite, (b) Fe_3O_4, and (c) BMNC.

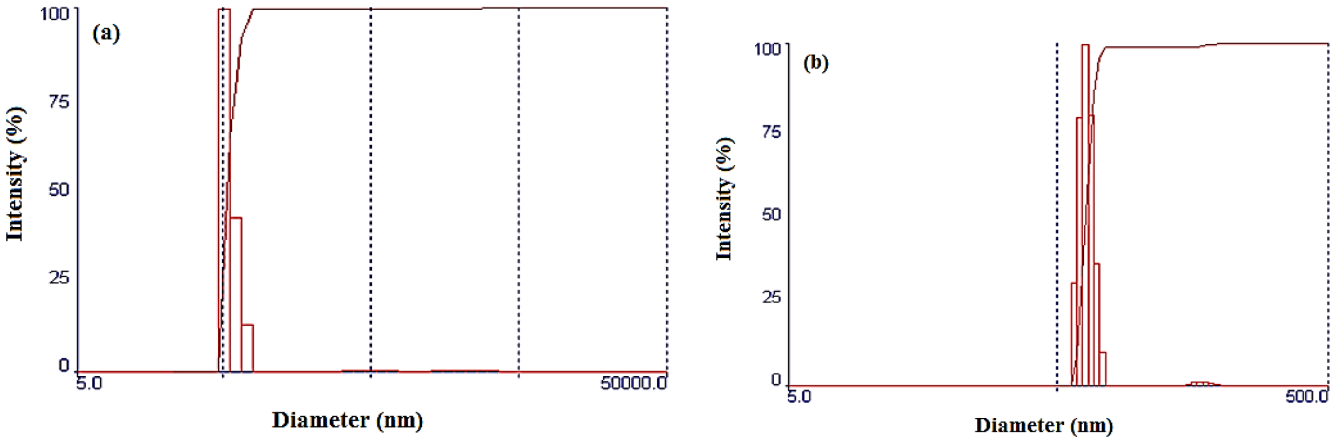

Fig. 4. DLS analysis of (a) Bentonite and (b) BMNC.

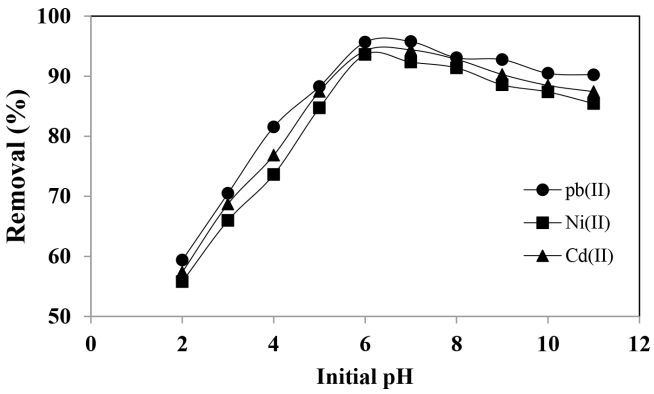

Fig. 5. The effect of pH on the removal of cadmium, nickel, and lead ions (conditions: contact time, 60 min; initial ion concentration, 5 mg/L; adsorbent dose, 1 g/L; temperature, 25°C; and speed mixing, 200 rpm).

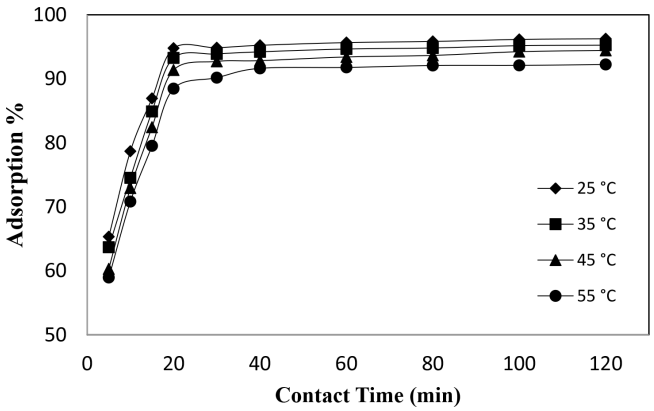

Fig. 6. The effects of time and temperature on the adsorption of lead ions (conditions: pH, 6; initial concentration of metallic ions, 5 mg/L; adsorbent dosage, 1 g/L; temperature, 25°C; and mixing speed, 200 rpm).

into a solution containing metal ions, the slope is high, and removal of metal ions increased from 0.25 to 2 g/L and after 2 g/L, figure dropped slightly different then the graph has a nearly fixed rate. At the adsorbent dosage of 2 g/L, the removal efficiencies of Pb, Cd, and Ni ions are obtained 98.32, 96.56,

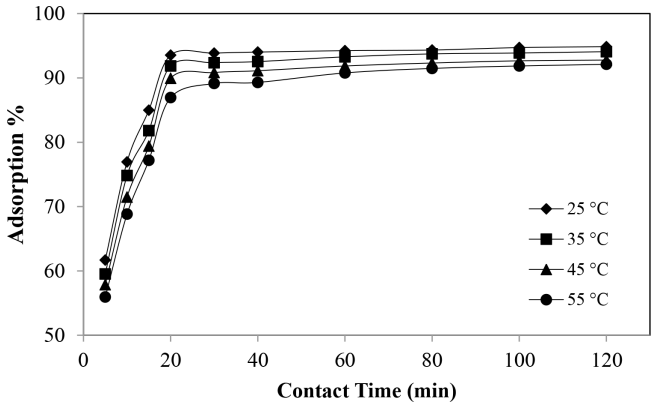

Fig. 7. The effects of time and temperature on the adsorption of cadmium ions (conditions: pH, 6; initial concentration of metallic ions, 5 mg/L; adsorbent dosage, 1 g/L; temperature, 25°C; and mixing speed, 200 rpm).

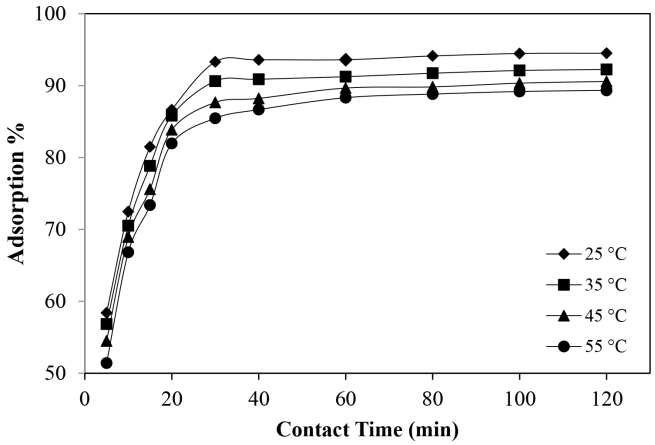

Fig. 8. The effects of time and temperature on the adsorption of nickel ions (conditions: pH, 6; initial concentration of metallic ions, 5 mg/L; adsorbent dosage, 1 g/L; temperature, 25°C; and mixing rate, 200 rpm).

and 94.66%, respectively. Increasing the slope of the graph at the beginning is due to a large number of active sites of magnetite adsorbent. In the later stages due to reducing the active sites available to adsorb metal ions, removal rate decreased.

The adsorption capacity of cadmium, lead, and nickel ions onto the BMNC is depicted in Fig. 11. As can be seen, the BMNC has a high adsorption capacity at low concentration and by increasing the adsorbent dosage, adsorption capability reduced. So, the best adsorbent concentration for the removal of Pb, Cd, and Ni ions was obtained 2 g/L.

3.6. Isotherm behavior of sorption

The adsorption capacity of Pb(II), Cd(II) and Ni(II), ions by the BMNC from synthetic wastewater was considered. Adsorption isotherms data were modeled using Langmuir, Freundlich, and Dubinin–Radushkevich (D–R) isotherms and the results are available in Table 3 and Figs. 12–14.

Langmuir model is based on this assumption which the adsorption occurs on the homogeneous surface. The Langmuir isotherm model can be written in the following form [5,19,24–27]:

$$\frac{C_e}{q_e} = \frac{1}{K_L q_m} + \frac{C_e}{q_m} \tag{3}$$

where q_e, C_e, K_L, and q_m are the amount of adsorbed metal ion in equilibrium state per gram of BMNC (mg/g), the equilibrium concentration of metal ions in solution (mg/L), the equilibrium constant related to the affinity of binding sites (L/mg) and the maximum amount of the Pb(II), Cd(II), and Ni(II) per mass of adsorbent (mg/g).

Freundlich isotherm also describes adsorption process where the adsorbent has a heterogeneous surface with sites that have different energies of adsorption. Eq. (2) presents the linearized form of this relation.

$$\ln q_e = \ln K_F + \frac{1}{n}\ln C_e \tag{4}$$

where K_F and n are the model constants showing the relationship between adsorption capacity and adsorption intensity, respectively.

Another useful isotherm is D–R model which is almost similar to Langmuir isotherm model [28]. The linear form of this model is as follows:

$$\ln q_e = \ln X_m - \beta\varepsilon^2 \tag{5}$$

In this equation, q_e, X_m (mol/g), β(mol²/J²) and ε are adsorbed metal ions per gram adsorbent, the maximum adsorption capacity, activity coefficient of adsorption energy, and the Polanyi potential, respectively. The amount of εis calculated as the following equation [28]:

$$\varepsilon = RT\ln\left(1 + \frac{1}{C_e}\right) \tag{6}$$

In Eq. (6), R and T are gas universal constant (J/mol k) and temperature (K), respectively.

β and X_m are obtained by plotting $\ln q_e$ against ε². Also, the adsorption energy is calculated from Eq. (7) [26]:

$$E = \frac{1}{\sqrt{2\beta}} \tag{7}$$

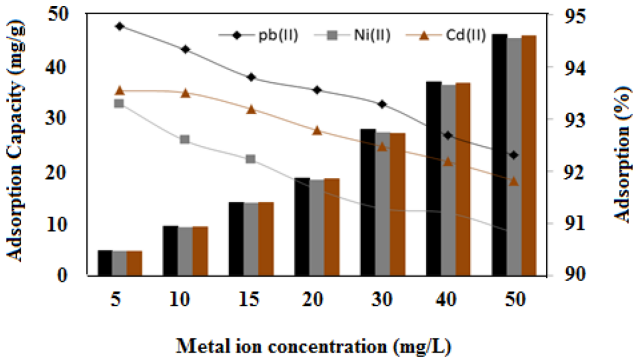

Fig. 9. The effect of initial concentration and adsorption capacity of cadmium, nickel, and lead ions (conditions: pH, 6; initial concentration of metallic ions, 5 mg/L; adsorbent dosage, 1 g/L; temperature, 25°C; and mixing speed, 200 rpm).

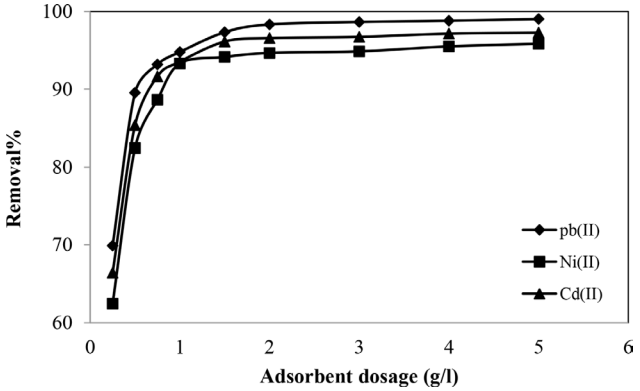

Fig. 10. The effect of BMNC on the removal percent of cadmium, nickel, and lead ions (conditions: pH, 6; initial concentration of metal ions, 5 mg/L; adsorbent dosage, 1 g/L; temperature, 25°C; and mixing speed, 200 rpm).

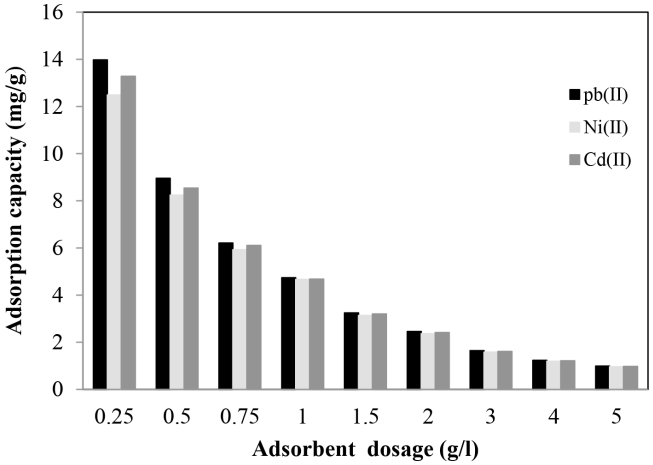

Fig. 11. The effect of adsorption capacity of BMNC on the removal of cadmium, nickel, and lead ions (conditions: pH, 6; initial concentration of metallic ions, 5 mg/L; adsorbent dosage, 1 g/L; temperature, 25°C; and mixing speed, 200 rpm).

Table 3
Langmuir, Freundlich, and Dubinin–Darushkevich isotherms constant for adsorption of Pb(II), Cd(II), and Ni(II) using BMNC from aqueous solutions

Isotherm	Parameters	Cadmium	Nickel	Lead
Langmuir	R^2	0.819	0.7735	**0.9585**
	R_L	0.18	0.1941	**0.5**
	q_{max}	9.4339	5.9808	**108.695**
	b	0.87	0.83	**0.2**
Freundlich	R^2	0.882	0.8353	**0.9597**
	n	1.018	0.913	**1.3**
	K_f	10.9091	8.6798	**12.92**
Dubinin–Radushkevich	R^2	0.956	0.941	**0.972**
	X_{max}	14.63	15.25	**11.68**
	E	2.34	1.92	**3.41**
	β (mol²/J²)	0.091	0.135	**0.043**

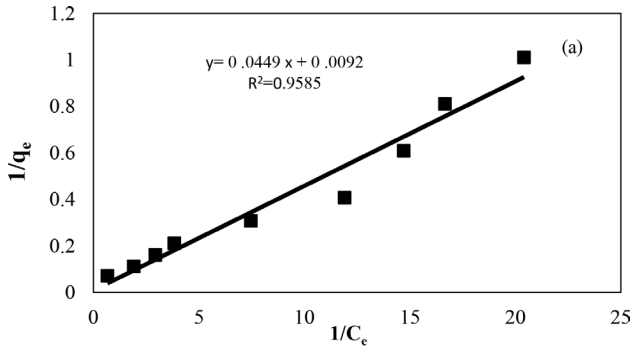

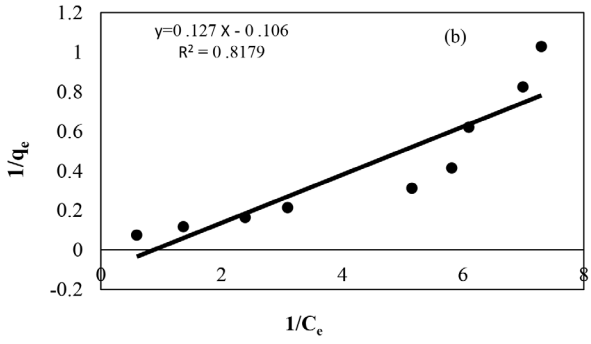

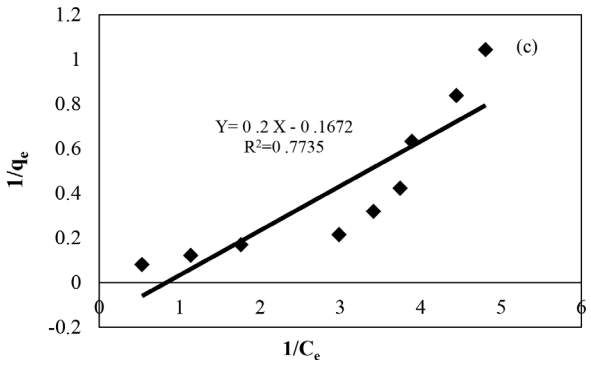

Fig. 12. Langmuir linear isotherm plots related to the adsorption of (a) Pb(II), (b) Cd(II), and (c) Ni(II) ions using BMNC from aqueous solutions.

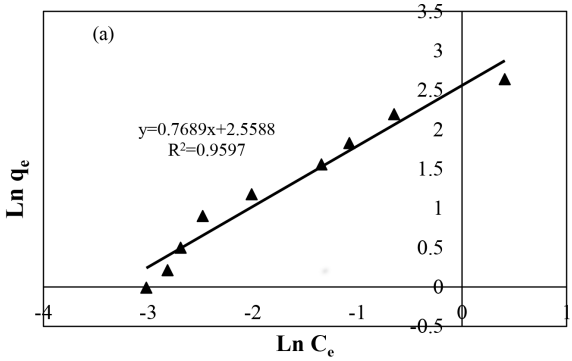

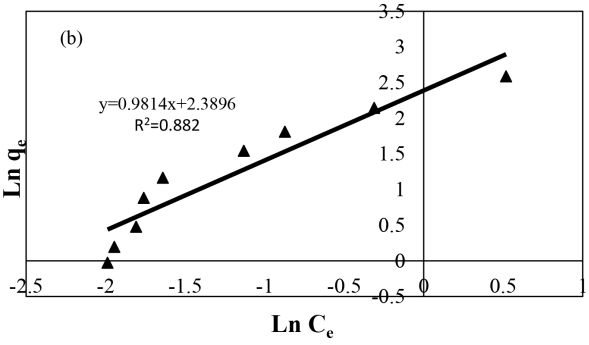

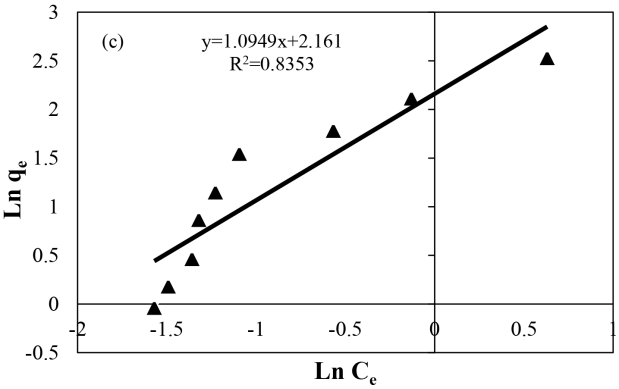

Fig. 13. Freundlich linear isotherm plots related to the adsorption of (a) Pb(II), (b) Cd(II), and (c) Ni(II) using BMNC from aqueous solutions.

The adsorption process is endothermic if the value of E is larger than 8. Also, $E < 8$ is indicating the adsorption process is physical and $8 < E < 16$ is shows that the adsorption process is occurred with ion exchange.

All the correlation coefficients, R^2, and the constants obtained from the models are given in Table 3 and they show the D–R isotherm is more proper to describe the adsorption equilibrium of Pb(II), Cd(II), and Ni(II) ions by the adsorbent. Also, the amount of the adsorption energy for three ions of Cd, Ni, and Pb was obtained to be 2.34, 1.92, and 3.40, respectively, which indicating the adsorption process of three ions using BMNC is exothermic and physical. Additionally, the maximum bio-adsorption capacities by Langmuir model were 9.4339, 108.695, and 5.9808 mg/g for cadmium, lead, and nickel, respectively.

3.7. Kinetic of adsorption

Kinetic studies of adsorption processes show the interactions between metal ions in aqueous solution and the adsorbent. In this study, in order to explain adsorbent kinematic behavior, pseudo-first-order and pseudo-second-order kinetic models were applied to the data.

Pseudo-first-order model is defined as follows:

$$\ln(q_e - q_t) = \ln q_e - k_1 t \tag{8}$$

where q_e (mg/g) is adsorbed ion volume in equilibrium per each gram adsorbent, q_t (mg/g) is adsorbed ion volume per each gram adsorbent at time t and k_1 adsorption constant (1/min). The adsorption rate constant (k_1) is calculated through plotting ln (q_e–q_t) against t [5,26–27,29].

The linear form of pseudo-second-order model is as follows:

$$\frac{t}{q_t} = \frac{1}{k_2 q_e^2} + \frac{t}{q_e} \tag{9}$$

The first adsorption rate is determined using Eq. (10):

$$H = Kq_e^{\,2} \tag{10}$$

where k_2 is pseudo-second-order kinetic rate constant (g/mg.g) [5,26,27].

Linear graphs of pseudo-first-order and pseudo-second-order models for lead, cadmium, and nickel adsorption using BMNC are shown in Figs. 15 and 16, respectively. The pseudo-first-order and pseudo-second-order kinetic model constants for Pb(II), Cd(II), and Ni(II) ions are also summarized in Tables 5 and 6.

According to the determined rates for correlation coefficient (R^2), it was shown that pseudo-second-order kinetic model was better to describe the kinetic behavior of Pb(II), Cd(II), and Ni(II) ions adsorption.

Also, there are a significant difference between calculated adsorption capacity using the pseudo-first-order kinetic model ($q_{e\cdot\text{cal}}$) and experimental data ($q_{e\cdot\text{exp}}$) in all temperatures (according to Table 4), So, the model is not suitable to describe the ability of adsorption kinetic. But according to Table 5, the values of $q_{e\cdot\text{cal}}$ using pseudo-second-order kinetic model have a very good matching with experimental data ($q_{e\cdot\text{exp}}$).

3.8. Thermodynamic study

The values of the thermodynamic parameters such as changes in Gibbs free energy ($\Delta G°$), enthalpy ($\Delta H°$), and entropy ($\Delta S°$) were determined by using the following equations and presented in Table 6 [5,24–26].

$$\Delta G° = -RT\ln K_c \tag{11}$$

$$\frac{\Delta S^\circ}{R} - \frac{\Delta H^\circ}{RT} = \ln K_c = \frac{-\Delta G^\circ}{RT} \tag{12}$$

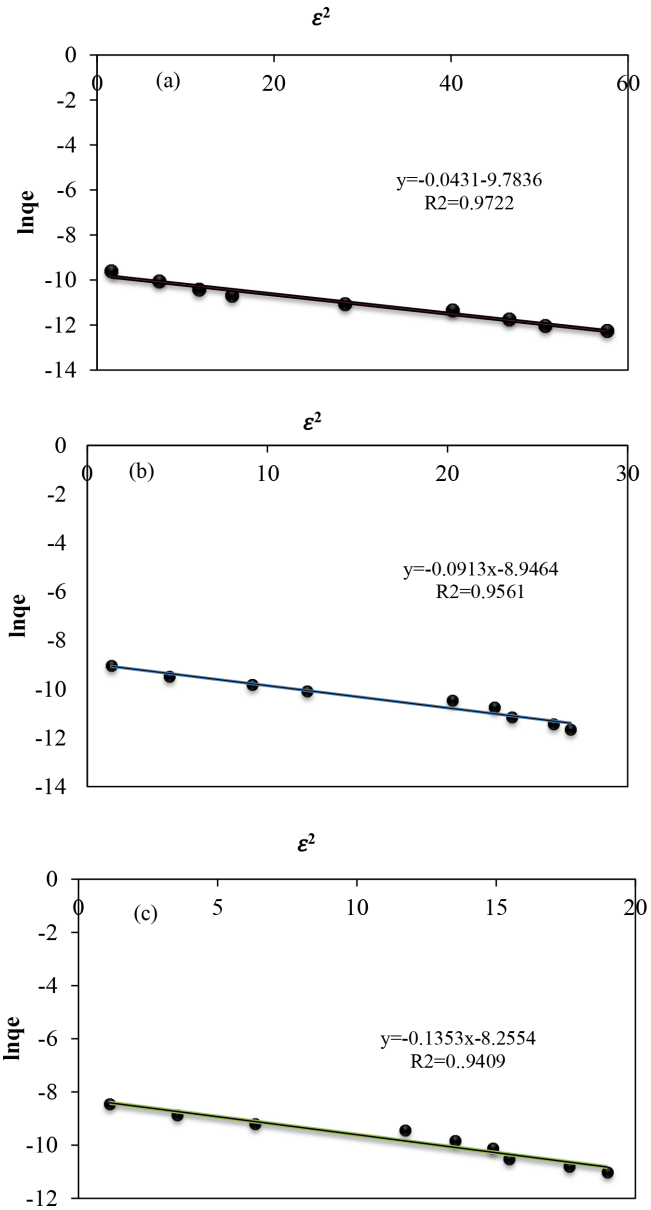

Fig. 14. Dubinin–Radushkevich isotherm plots related to the adsorption of (a) Pb(II), (b) Cd(II), and (c) Ni(II) using BMNC from aqueous solutions.

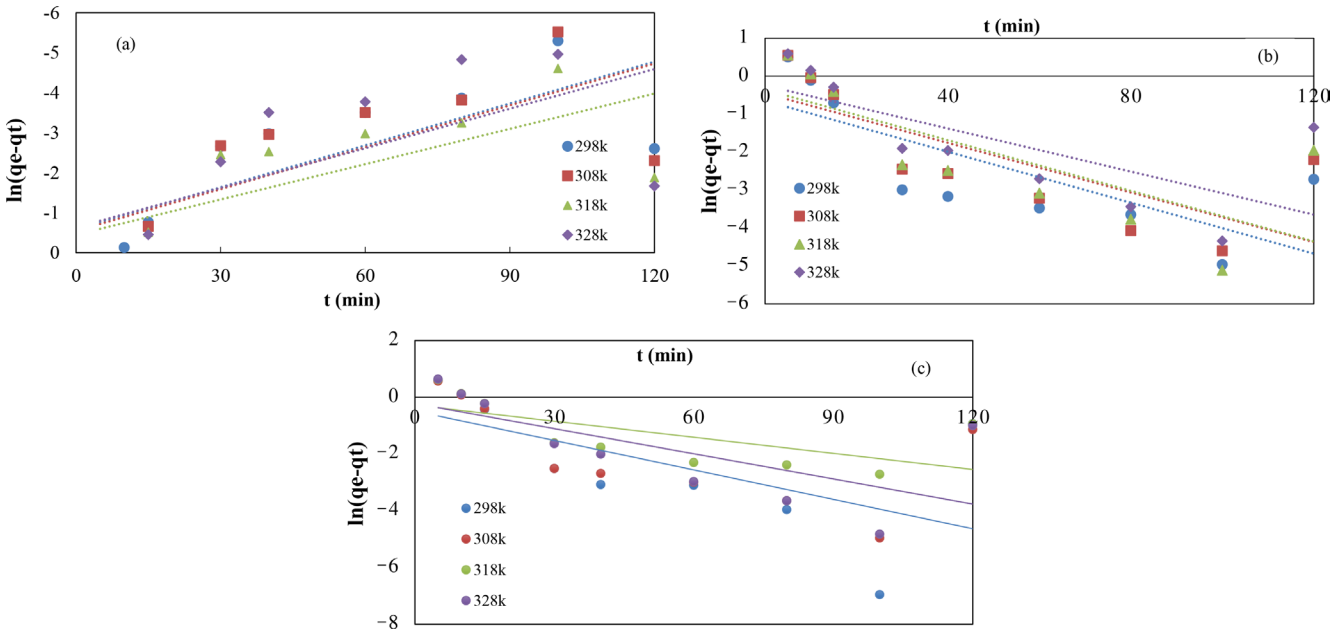

Fig. 15. Pseudo-first-order kinetic model plots related to the adsorption of (a) Pb(II), (b) Cd(II), and (c) Ni(II) ions.

Table 4
Pseudo-first-order kinematic model constants for the adsorption of Pb(II), Cd(II), and Ni(II) using BMNC

Pseudo-first-order kinetic model				
Temperature (*K*)	$q_{e.exp}$ (mg/g)	K_1(1/min)	$q_{e.cal}$ (mg/g)	R^2
Cadmium				
298.15	4.743	0.0336	0.5225	**0.5756**
308.15	4.704	0.0498	0.8796	**0.8573**
318.15	4.639	0.0529	1.0607	**0.8955**
328.15	4.606	0.0479	1.2504	**0.9277**
Lead				
298.15	4.813	0.0349	0.5583	**0.5952**
308.15	4.763	0.0349	0.5809	**0.5495**
318.15	4.722	0.6370	0.6370	**0.5232**
328.15	4.612	0.5307	0.5307	**0.4347**
Nickel				
298.15	4.725	0.0364	0.6142	**0.3633**
308.15	4.612	0.028	0.5870	**0.3934**
318.15	4.853	0.0189	0.7572	**0.4265**
328.15	4.467	0.0295	0.8026	**0.4482**

where $\Delta G°$, $\Delta H°$, and $\Delta S°$ are in terms of KJ/mol, KJ.mol, and J/mol.K, respectively. Also, R and T are the universal gas constant, 8.314 (J/mol K) and the absolute temperature (K).

The apparent equilibrium constant K_c of the adsorption is defined as follows:

$$K_c = \frac{C_{ad,eq}}{C_{eq}} \tag{13}$$

$C_{ad,eq}$ and C_{eq} are the amount of dye adsorbed on the adsorbent at equilibrium (mg/L) and the equilibrium concentration of dye in the solution (mg/L), respectively. In this case, the activity should be used instead of concentration in order to obtain the standard thermodynamic equilibrium constant (K_c) of the adsorption system [30].

Gibbs free energy in all four temperatures 25°C, 35°C, 45°C, and 55°C for three ions of lead, nickel, and cadmium is negative. This negative result indicates that the adsorption process three ions amounts of lead, nickel,

Table 5
Pseudo-second-order synthetic model constants for the adsorption of Pb(II), Cd(II), and Ni(II) ions using BMNC

Pseudo-second-order kinetic model				
Temperature (*K*)	(mg/g) $q_{e.exp}$	K_2(1/min)	$q_{e.cal}$(mg/g)	R^2
Cadmium				
298.15	4.743	0.12	4.8262	**0.9997**
308.15	4.704	0.1005	4.8030	**0.9997**
318.15	4.639	0.09088	4.8473	**0.9996**
328.15	4.606	0.07554	4.7303	**0.9997**
Lead				
298.15	4.813	0.1251	4.8923	**0.9998**
308.15	4.763	0.11054	4.8543	**0.9997**
318.15	4.722	0.0955	4.8216	**0.9997**
328.15	4.612	0.095	4.7214	**0.9996**
Nickel				
298.15	4.725	0.08317	4.8473	**0.9997**
308.15	4.612	0.08419	4.7281	**0.9997**
318.15	4.583	0.0703	4.6838	**0.9997**
328.15	4.467	0.06845	4.6082	**0.9997**

Table 6
Thermodynamic properties for the adsorption of Pb(II), Ni(II), and Cd(II) ions using BMNC

Ions	Δ*H*°(KJ/mol)	Δ*S*°(J/mol.K)	ΔG°(KJ/mol)			
			298.15K	308.15K	318.15K	328.15K
Lead	–2.9705	19.2194	–7.1824	–6.7277	–6.2418	–5.5540
Nickel	–2.8941	20.3435	–6.5251	–5.8076	–5.1835	–4.8279
Cadmium	–3.3048	19.0033	–6.6218	–6.2056	–5.7913	–5.1692

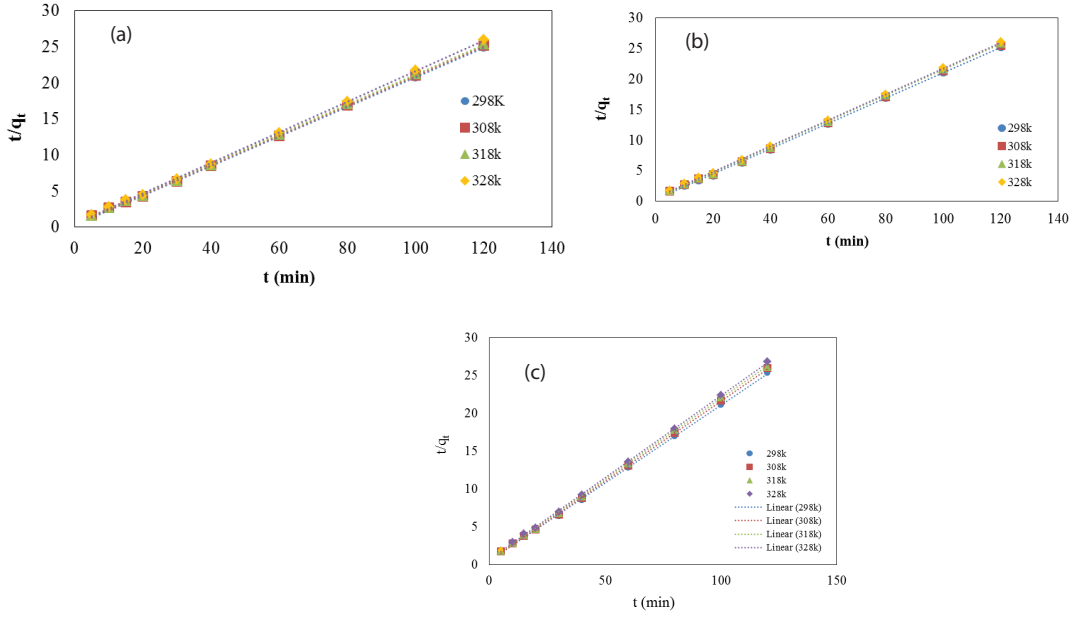

Fig. 16. Pseudo-second-order kinetic model plots related to the adsorption of (a) Pb(II), (b) Cd(II), and (c) Ni(II) ions.

and cadmium with BMNC adsorbent is the possible and spontaneous.

Enthalpy value obtained for three ions of lead, nickel, and cadmium with the adsorbent is negative. The negative values infer that the adsorption process three ions of lead, nickel, and cadmium using the BMNC is exothermic.

The resulting entropy for three ions of lead, nickel, and cadmium using this adsorbent is positive. These positive values indicate that the adsorption process of lead, nickel, and cadmium ions using the BMNC is irreversible.

4. Conclusions

This work is to survey the impact of bentonite/Fe_3O_4 nanocomposite on the removal of Pb(II), Cd(II), and Ni(II) from aqueous solution. To characterize the adsorbent properties, the analysis of SEM, FTIR, BET, XRD, XRF, and DLS were done. To this end, the effect of important parameters like contact time, pH, sorbent dosage, temperature, and the initial concentration of metal ions were checked. The results cleared that the optimal pH of all three metal ions is obtained 6.

After determining the optimal pH, optimal contact time of Cd and Pb ions determined 20 min and nickel ion calculated 30 min. Also, the best conditions for initial ion concentration, BMNC dosage, and temperature were determined 5 mg/L, 3 g/L, and 25°C, respectively. Of the three models mentioned isotherm, D–R model was more favorable than Langmuir and Freundlich models due to the higher correlation coefficient. In addition, two pseudo-first-order and pseudo-second-order kinematic models were evaluated in which pseudo-second-order model was more appropriate to investigate the kinetic behavior of BMNC adsorbent. Moreover, the thermodynamic behavior of metal ions was studied. The results represent that the Gibbs free energy, enthalpy, and entropy are negative, negative, and positive, which show adsorption process of these metal ions using BMNC adsorbent is spontaneous, exothermic, and irreversible.

Disclosure statement

No potential conflict of interest was reported by the authors.

References

[1] F. Fu, Q. Wang, Removal of heavy metal ions from wastewaters: a review, J. Environ. Manage., 92 (2011) 407–418.
[2] M.K. Bojdi, M.H. Mashhadizadeh, M. Behbahani, A. Farahani, S.S. Hosseini Davarani, A. Bagheri, Synthesis, characterization and application of novel lead imprinted polymer nanoparticles as a high selective electrochemical sensor for ultra-trace determination of lead ions in complex matrixes, Electrochim. Acta, 136 (2014) 59–65.
[3] A.H.A. El Hameed, W.E. Eweda, K.A.A. Abou-Taleb, H.I. Mira, Biosorption of uranium and heavy metals using some local fungi isolated from phosphatic fertilizers, Ann. Agric. Sci., 60 (2015) 345–351.
[4] H.A. Aziz, M.N. Adlan, C.S. Hui, M.S.M. Zahari, B.H. Hameed, Removal of Ni, Cd, Pb, Zn and colour from aqueous solution using potential low cost adsorbent, Indian J. Eng. Mater. Sci., 12 (2005) 248–258.
[5] F. Shakerian Khoo, H. Esmaeili, Synthesis of CaO/Fe_3O_4 magnetic composite for the removal of Pb(II) and Co(II) from synthetic wastewater, J. Serb. Chem. Soc., 83 (2018) 237–249. doi: doi.org/10.2298/JSC170704098S.
[6] S. Hashemian, $MnFe_2O_4$/bentonite nano-composite as a novel magnetic material for adsorption of acid red 138, Afr. J. Biotechnol., 9 (2010) 8667–8671.
[7] S. Hashemian, A. Foroghimoqhadam, Effect of copper doping on $CoTiO_3$ ilmenite type nanoparticles for removal of congo red from aqueous solution, Chem. Eng. J., 235 (2014) 299–306.
[8] M.K. Uddin, A review on the adsorption of heavy metals by clay minerals, with special focus on the past decade, Chem. Eng. J., 308 (2017) 438–462.
[9] H. Esmaeili, R. Foroutan, Investigation into ion exchange and adsorption methods for removing heavy metals from aqueous solutions, Int. J. Biol. Pharmacol. Allied Sci., 4 (2015) 620–629.
[10] R. Foroutan, H. Esmaeili, M. Kosari Fard, Equilibrium and kinetic studies of Pb(II) biosorption from aqueous solution using shrimp peel, Int. Res. J. Appl. Basic Sci., 9 (2015) 1954–1965.
[11] R.D. Ambashta, M. Sillanpää, Water purification using magnetic assistance: a review, J. Hazard. Mater., 180 (2010) 38–49.
[12] T.A. Saleh, V.K. Gupta, Photo-catalyzed degradation of hazardous dye methyl orange by use of a composite catalyst consisting of multi-walled carbon nanotubes and titanium dioxide, J. Colloid Interface Sci., 371 (2012) 101–106.
[13] M. Rossier, M. Schreier, U. Krebs, B. Aeschlimann, R. Fuhrer, M. Zeltner, R.N. Grass, D. Günther, W.J. Stark, Scaling up magnetic filtration and extraction to the ton per hour scale using carbon coated metal nanoparticles, Sep. Purif. Technol., 96 (2012) 68–74.
[14] X. Zhao, L. Lv, B. Pan, W. Zhang, S. Zhang, Q. Zhang, Polymer-supported nanocomposites for environmental application: a review, Chem. Eng. J., 170 (2011) 381–394.
[15] A.M. Muliwa, T.Y. Leswifi, M.S. Onyango, A. Maity, Magnetic adsorption separation (MAS) process: an alternative method of extracting Cr(VI) from aqueous solution using polypyrrole coated Fe_3O_4 nanocomposites, Sep. Purif. Technol., 158 (2016) 250–258.
[16] S. Hashemian, H. Saffari, S. Ragabion, Adsorption of cobalt (II) from aqueous solutions by Fe_3O_4/bentonite nanocomposite, Water Air Soil Pollut., 226 (2015) 2212.
[17] M. Galamboš, P. Suchánek, O. Rosskopfová, Sorption of anthropogenic radionuclides on natural and synthetic inorganic sorbents, J Radiol. Nucl. Chem., 293 (2012) 613–633.
[18] M. Kaur, M. Singh, S.S. Mukhopadhyay, D. Singh, M. Gupta, Structural, magnetic and adsorptive properties of clay ferrite nanocomposite and its use for effective removal of Cr(VI) from water, J. Alloys Compd., 653 (2015) 202–211.
[19] M.E. Mahmoud, A.A. Yakout, K.H. Hamza, M.M. Osman, Novel nano-Fe_3O_4-encapsulated-dioctylphthalate and linked-triethylenetetramine sorbents for magnetic solid phase removal of heavy metals, J. Ind. Eng. Chem., 25 (2015) 207–215.
[20] M.E. Mahmoud, M.S. Abdelwahab, E.M. Fathallah, Design of novel nano-sorbents based on nano-magnetic iron oxide–bound-nano-silicon oxide–immobilized-triethylenetetramine for implementation in water treatment of heavy metals, Chem. Eng. J., 223 (2013) 318–327.
[21] L.G. Yan, K. Yang, R.R. Shan, T. Yan, J. Wei, S.J. Yu, H.Q. Yu, B. Du, Kinetic, isotherm and thermodynamic investigations of phosphate adsorption onto core–shell Fe 3 O 4@ LDHs composites with easy magnetic separation assistance, J. Colloid Interface Sci., 448 (2015) 508–516.
[22] R. Foroutan, H. Esmaeili, M. Abbasi, M. Rezakazemi, M. Mesbah, Adsorption behavior of Cu(II) and Co(II) using chemically modified marine algae, Environ. Technol., 52 (2017). doi: 10.1080/09593330.2017.1365946.
[23] L. Nemeş, L. Bulgariu, Optimization of process parameters for heavy metals biosorption onto mustard waste biomass, Open Chem., 14 (2016) 175–187.
[24] A. Teimouri, H. Esmaeili, R. Foroutan, B. Ramavandi, Adsorptive performance of calcined *Cardita bicolor* for attenuating Hg(II) and As(III) from synthetic and real wastewaters, Korean J. Chem. Eng., 35 (2017) 479–488. doi: https://doi.org/10.1007/s11814-017-0311-y.
[25] L. Bulgariu, M. Lupea, D. Bulgariu, C. Rusu, M. Macoveanu, Equilibrium study of Pb(II) and Cd(II) biosorption from aqueous solution on marine green algae biomass, Environ. Eng. Manage. J., 12 (2013) 183–190.

[26] F. Saberzadeh Sarvestani, H. Esmaeili, B. Ramavandi, Modification of *Sargassum angustifolium* by molybdate during a facile cultivation for high-rate phosphate removal from wastewater: structural characterization and adsorptive behavior, 3 Biotech, 6 (2016) 251.
[27] R. Foroutan, H. Esmaeili, S.M. Derakhshandeh Rishehri, F. Sadeghzadeh, S.R. Mirahmadi, M. Kosarifard, B. Ramavandi, Zinc, nickel, and cobalt ions removal from aqueous solution and plating plant wastewater by modified *Aspergillus flavus* biomass: a data set, Data Brief, 12 (2017) 485–492.
[28] G. Nacu, D. Bulgariu, M.C. Popescu, M. Harja, D.T. Juravle, L. Bulgariu, Removal of Zn(II) ions from aqueous media on thermal activated sawdust, Desal. Wat. Treat., 57 (2016) 21904–21915.
[29] A. Sari, M. Tuzen, D. Citak, M. Soylak, Equilibrium, kinetic and thermodynamic studies of adsorption of Pb(II) from aqueous solution onto Turkish kaolinite clay, J. Hazard Mater., 149 (2007) 283–291.
[30] M. Dundar, C. Nuhoglu, Y. Nuhoglu, Biosorption of Cu(II) ions onto the litter of natural trembling poplar forest, J. Hazard Mater., 151 (2008) 86–95.